14. Dainichi T, Uchi H, Moroi Y, Furue M. Stevens-Johnson syndrome, drug-induced hypersensitivity syndrome and toxic epidermal necrolysis caused by allopurinol in patients with a common HLA allele: what causes the diversity? Dermatology 2007; 215:86-8.
15. Hung SI, Chung WH, Liou LB, Chu CC, Lin M, Huang HP, et al. HLA-B*5801 allele as a genetic marker for severe cutaneous adverse reactions caused by allopurinol. Proc Natl Acad Sci U S A 2005;102:4134-9.
16. Lonjou C, Borot N, Sekula P, Ledger N, Thomas L, Halevy S, et al. A European study of HLA-B in Stevens-Johnson syndrome and toxic epidermal necrolysis related to five high-risk drugs. Pharmacogenet Genomics 2008;18:99-107.
17. Lonjou C, Thomas L, Borot N, Ledger N, de Toma C, LeLouet H, et al. A marker for Stevens-Johnson syndrome.: ethnicity matters. Pharmacogenomics J 2006;6:265-8.
18. Mondino BJ, Brown SI, Biglan AW. HLA antigens in Stevens-Johnson syndrome with ocular involvement. Arch Ophthalmol 1982;100:1453-4.
19. Power WJ, Saidman SL, Zhang DS, Vamvakas EC, Merayo-Lloves JM, Kaufman AH, et al. HLA typing in patients with ocular manifestations of Stevens-Johnson syndrome. Ophthalmology 1996;103:1406-9.
20. Roujeau JC, Bracq C, Huyn NT, Chaussalet E, Raffin C, Duedari N. HLA phenotypes and bullous cutaneous reactions to drugs. Tissue Antigens 1986;28:251-4.
21. Roujeau JC, Huynh TN, Bracq C, Guillaume JC, Revuz J, Touraine R. Genetic susceptibility to toxic epidermal necrolysis. Arch Dermatol 1987;123:1171-3.
22. Araki Y, Sotozono C, Inatomi T, Ueta M, Yokoi N, Ueda E, et al. Successful treatment of Stevens-Johnson syndrome with steroid pulse therapy at disease onset. Am J Ophthalmol 2009;147:1004-11, e1.
23. Sotozono C, Ang LP, Koizumi N, Higashihara H, Ueta M, Inatomi T, et al. New grading system for the evaluation of chronic ocular manifestations in patients with Stevens-Johnson syndrome. Ophthalmology 2007;114:1294-302.
24. Ueta M, Sotozono C, Inatomi T, Kojima K, Hamuro J, Kinoshita S. Association of IL4R polymorphisms with Stevens-Johnson syndrome. J Allergy Clin Immunol 2007;120:1457-9.
25. Ueta M, Sotozono C, Inatomi T, Kojima K, Hamuro J, Kinoshita S. Association of combined IL-13/IL-4R signaling pathway gene polymorphism with Stevens-Johnson syndrome accompanied by ocular surface complications. Invest Ophthalmol Vis Sci 2008;49:1809-13.
26. Ueta M, Sotozono C, Inatomi T, Kojima K, Hamuro J, Kinoshita S. Association of Fas Ligand gene polymorphism with Stevens-Johnson syndrome. Br J Ophthalmol 2008;92:989-91.
27. Ueta M, Sotozono C, Tokunaga K, Yabe T, Kinoshita S. Strong association between HLA-A*0206 and Stevens-Johnson syndrome in the Japanese. Am J Ophthalmol 2007;143:367-8.
28. Ueta M, Tokunaga K, Sotozono C, Inatomi T, Yabe T, Matsushita M, et al. HLA class I and II gene polymorphisms in Stevens-Johnson syndrome with ocular complications in Japanese. Mol Vis 2008;14:550-5.
29. Nakano M, Ikeda Y, Taniguchi T, Yagi T, Fuwa M, Omi N, et al. Three susceptible loci associated with primary open-angle glaucoma identified by genome-wide association study in a Japanese population. Proc Natl Acad Sci U S A 2009;106: 12838-42.
30. Auquier-Dunant A, Mockenhaupt M, Naldi L, Correia O, Schroder W, Roujeau JC. Correlations between clinical patterns and causes of erythema multiforme majus, Stevens-Johnson syndrome, and toxic epidermal necrolysis: results of an international prospective study. Arch Dermatol 2002;138:1019-24.
31. Bastuji-Garin S, Rzany B, Stern RS, Shear NH, Naldi L, Roujeau JC. Clinical classification of cases of toxic epidermal necrolysis, Stevens-Johnson syndrome, and erythema multiforme. Arch Dermatol 1993;129:92-6.
32. Yamane Y, Aihara M, Ikezawa Z. Analysis of Stevens-Johnson syndrome and toxic epidermal necrolysis in Japan from 2000 to 2006. Allergol Int 2007;56:419-25.
33. Kojima K, Ueta M, Hamuro J, Hozono Y, Kawasaki S, Yokoi N, et al. Human conjunctival epithelial cells express functional Toll-like receptor 5. Br J Ophthalmol 2008;92:411-6.
34. Ueta M, Hamuro J, Kiyono H, Kinoshita S. Triggering of TLR3 by polyI: C in human corneal epithelial cells to induce inflammatory cytokines. Biochem Biophys Res Commun 2005;331:285-94.
35. Ueta M, Matsuoka T, Narumiya S, Kinoshita S. Prostaglandin E receptor subtype EP3 in conjunctival epithelium regulates late-phase reaction of experimental allergic conjunctivitis. J Allergy Clin Immunol 2009;123:466-71.
36. Matsuoka T, Narumiya S. Prostaglandin receptor signaling in disease. Sci World J 2007;7:1329-47.
37. Narumiya S. Prostanoids and inflammation: a new concept arising from receptor knockout mice. J Mol Med 2009;87:1015-22.
38. Honda T, Matsuoka T, Ueta M, Kabashima K, Miyachi Y, Narumiya S. Prostaglandin E(2)-EP(3) signaling suppresses skin inflammation in murine contact hypersensitivity. J Allergy Clin Immunol 2009;124:809-18, e2.
39. Narumiya S, Sugimoto Y, Ushikubi F. Prostanoid receptors: structures, properties, and functions. Physiol Rev 1999;79:1193-226.

METHODS

GWAS

We used the Affymetrix GeneChip Mapping 500K Array Set in the GWAS. In brief, 2 aliquots of approximately 250 ng of genomic DNA were digested with *Nsp*I and *Sty*I. Adaptor oligonucleotides specific to each digested end were ligated to the fragments, and the resulting molecules were amplified by means of PCR with adaptor-specific primers. The PCR products were fragmented, labeled, and hybridized with the corresponding *Nsp*I or *Sty*I arrays. After hybridization, the arrays were stained and scanned with a GeneChip Scanner 3000. The scanned data were managed with GeneChip Operating Software. Intensity data provided by the CEL files were used for SNP genotyping. Detailed methods for the genotype-calling algorithms, SNP genotyping, and criteria for SNP selection are described below.

SNP genotyping. The SNPs were initially genotyped with the Dynamic Model algorithm with GeneChip Genotyping Analysis Software (GTYPE, Affymetrix) to check the quality of each array. Arrays that did not pass a call rate of 93% at a confidence threshold of 0.33 were rehybridized with the stored hybridization cocktail. To confirm that no samples were mixed up, we checked the genotypes of 50 common SNPs placed on both the *Nsp*I and *Sty*I arrays. We checked for sex mismatch by comparing clinical records and genotyping results for the X-chromosome. For the association analysis, we genotyped the SNPs by using the Bayesian Robust Linear Model with a Mahalanobis distance classifier (BRLMM) algorithm with a BRLMM Analysis Tool. The multiple sample classification was performed by clustering 60 case and 301 control samples, separately. Because 60 samples were not enough for accurate clustering, we added 286 population-matched samples from another project (data not shown). After excluding a sample from the control group that yielded low-quality data (see the Results section), we used 60 case and 300 control samples for the association analysis.

Criteria for SNP selection. From 500,568 SNPs (262,264 and 238,304 SNPs in the *Nsp*I and *Sty*I arrays, respectively), a total of 313,924 autosomal SNPs were selected for association analysis based on our stringent QC filter, which had the following criteria: (1) 90% or greater call rate per SNP in cases and control subjects, (2) 5% or less call rate difference between cases and control subjects for each SNP, and (3) 5% or greater minor allele frequency (MAF) in cases and control subjects. After the association analysis, we visually checked the 2-dimensional cluster plots of the genotypes for the 25 SNPs that passed the FDR threshold to remove the SNPs that clustered poorly. Using our custom tool, we selected the SNPs with good 2-dimensional cluster plots, as described below. The cluster for each SNP was given an acceptability score of 0 (reject), 1 (acceptable), or 2 (accept), and this was done separately for the case and control data. The clusters were scored in random order by 3 independent observers (M. N., T. T., and K. T.). The score given by at least 2 observers had to agree to be accepted and was expressed as a total acceptability score of the summed case and control scores, ranging from 0 to 4. We excluded poorly clustered SNPs, which were given a total score of 0 to 3. We ultimately selected 3 SNPs from the GWAS as candidates (Table I).

Fine-mapping of the SNPs in the *EP3* region

Genotyping of the SNPs in *EP3* was performed by using the iSelect Custom Infinium Genotyping system (iSelect, Illumina). Briefly, 150 to 300 ng of genomic DNA was denatured and amplified by using the manufacturer-provided reagents. The samples were then fragmented, precipitated, and resuspended completely. After being denatured, the samples were hybridized with iSelect Genotyping BeadChips, and the BeadChips were then reacted to detect single-base or allele-specific extensions. After being stained, the BeadChips were scanned with a BeadArray Reader. The intensity data from each chip were entered for analysis by using the BeadStudio 3.0 software, which converts fluorescence intensities into SNP genotyping results. Detailed methods for the SNP selection, SNP genotyping, and criteria for SNP selection are described below.

SNP selection. We genotyped the SNPs in the *EP3* gene using 75 case samples, including 60 from the GWAS population, and 455 control samples from different subjects than in the GWAS by using the iSelect Custom Infinium Genotyping system (iSelect, Illumina). We first selected the SNPs on the *EP3* gene together with adjacent SNPs on the LD block of the HapMap-JPT and HapMap-CHB populations derived from the UCSC Genome Browser (http://genome.ucsc.edu/cgi-bin/hgGateway). Of these, we selected the non-monomorphic SNPs in the HapMap-JPT and HapMap-CHB populations. We then validated the suitability of selected SNPs for constructing custom chips by using the Assay Design Tool. Finally, 163 SNPs were chosen for the custom chip and used for the subsequent analysis. To check sex mismatches between the clinical records and the genotyping results, we also analyzed 13 SNPs on the X-chromosome.

SNP genotyping. To check the quality of each data point, the SNPs were initially genotyped by clustering 530 (75 cases plus 455 control subjects) samples at a no-call threshold of 0.15. For these SNPs, we analyzed the call rate per sample and the QC indices (staining, extension, target removal, hybridization, stringency, nonspecific binding, and nonpolymorphic) using the BeadStudio software. Because 8 samples showed a lower call rate than the others (<95%), we reprocessed them starting with the sample preparation, as described in the manufacturer's technical note (Infinium Genotyping Data Analysis). All the reprocessed samples showed a higher call rate than was seen in the initial results. We excluded 7 samples (see the Results section) and then clustered the results from 75 case and 448 control samples separately by using our standard cluster file (data not shown). Three independent observers (M. N., T. T., and T. Y.) visually checked the 2-dimensioanl cluster plots of the genotypes for all of the SNPs.

Criteria for SNP selection. From the 163 SNPs, 86 were selected for the association analysis based on our QC filter: (1) 90% or greater call rate per SNP and (2) 5% or greater MAF for both cases and control subjects.

SNP analysis by means of direct sequencing

The 6 SJS/TEN-associated SNPs that showed significant associations ($P < .01$) in the Custom Genotyping BeadChip assay were sequenced from both sides (ie, the forward and reverse directions) for rigorous assessment of our genotyping results. For the *EP3* SNPs, the PCR and sequence primers were as shown in Table E2. Genomic DNA was isolated from human peripheral blood at SRL, Inc (Tokyo, Japan). PCR amplification was performed with DNA polymerase (Takara, Shiga, Japan) for 35 cycles at 94°C for 1 minute, 60°C for 1 minute, and 72°C for 1 minute on a commercial PCR machine (GeneAmp, Perkin-Elmer Applied Biosystems). The PCR products were reacted with BigDye Terminator v3.1 (Applied Biosystems), and the sequence reactions were resolved on an ABI PRISM 3100 Genetic Analyzer (Applied Biosystems).

PHCjE cells

PHCjE cells were cultured for use in ELISAs. Conjunctival tissues were washed and immersed for 1 hour at 37°C in 1.2 U/mL purified dispase (Roche Diagnostic Ltd, Basel, Switzerland). The epithelial cells were detached, collected, and cultured in low-calcium k-SFM medium supplemented with 0.2 ng/mL human recombinant epidermal growth factor (Invitrogen, Carlsbad, Calif), 25 mg/mL bovine pituitary extract (Invitrogen), and 1% antibiotic-antimycotic solution. Cell colonies usually became obvious within 3 to 4 days. After reaching 80% confluence in 7 to 10 days, the cells were seeded into culture dishes and used for experiments once they had reached subconfluence.

Immunohistochemistry

Sections 6 μm thick were cut and fixed in 100% acetone at 4°C for 10 minutes. They were then blocked for 30 minutes with 10% normal donkey serum in PBS. The anti-EP3 antibody was a rabbit polyclonal antibody (Cayman Chemical Co, Ann Arbor, Mich). A nonspecific rabbit IgG (Abcam Ltd, Cambridge, United Kingdom) was used as the negative control. The secondary antibody (Biotin-SP–conjugated AffiniPure F[ab′]$_2$ Fragment Donkey Anti-Rabbit IgG[H+L], 1:500 dilution; Jackson ImmunoResearch, Baltimore, Md) was applied for 30 minutes. Vectastain ABC Reagent (Vector Laboratories, Inc, Burlingame, Calif) was used to amplify the signal from the DAB substrate (DAB substrate kit, Vector Laboratories).

RESULTS

Power estimation

As described in the introduction, it is extremely difficult to recruit patients with SJS accompanied by ocular complications because of the low annual rate of incidence. Therefore we decided to complete the GWAS using the first set of subjects (60 cases vs 300 control subjects) and then move on to the fine-mapping analysis by adding the new samples. In support of that decision, we estimated the statistical power of both situations: 100 cases versus 756 control subjects, which would be the maximum number of subjects throughout the study, and 60 cases versus 300 control subjects (Fig E3). If we expected to detect SNPs with an MAF of 0.1 and an odds ratio of 1.5 at a less than .05, the power of both situations were 0.46 (blue line) and 0.30 (grey line), respectively. The results suggested that even if we performed the GWAS with 100 cases and 756 control subjects, we could gain a statistical power of no more than twice that of the sample size we used. Therefore our decision was fairly reasonable considering the circumstances surrounding the collection of our samples.

Genotyping for GWAS

We first genotyped 60 case and 301 control samples using the Affymetrix GeneChip Mapping 500K Array Set. Using the Dynamic Model algorithm, we found no mix-ups of the samples between the *Nsp*I and *Sty*I arrays. We observed no inconsistent results for sex between the clinical records and the genotyping results. The final genotyping results for 500,568 SNPs were called by using the BRLMM algorithm. Because the value of the raw intensity of 1 control sample was out of the accepted range, this sample was excluded from the analysis. Ultimately, we used 60 cases and 300 control subjects for the association study. The mean call rate per sample was more than 98% for the case and control samples. Our stringent QC filter for the call rate and MAF (see the Methods section) permitted 313,924 autosomal SNPs to be used in the subsequent analysis.

Quantile-quantile plot

According to the quantile-quantile plot (Fig E4, *A*), the observed P value deviated from the expected P value between 10^{-2} and 10^{-3}, which might be reflecting the imbalanced sample number of our case-control population. When we analyzed the distribution with and without 44 SNPs from the *EP3* region (Fig E4, *B*), we were able to see a slight difference in the deviation (enlarged box, red open circle to black-filled circle), suggesting the contribution of the *EP3* region to the SJS trait. However, because the magnitude of the difference was small, the genetic contribution of *EP3* SNPs to the trait seemed to be shared by other unidentified variants, which should also be explained from the result of the GWAS that we could not obtain genome-wide significant SNPs possessing strong effects to the trait.

Population stratification of the subjects used in the GWAS

According to the population stratification analyses using STRUCTURE software, our case plus control samples showed a similar stratification with those of the HapMap-JPT population (Fig E5, *A*) and clearly differed from those of the HapMap-CEU and HapMap Yoruba in Nigeria populations (Fig 5, *A*). The analysis also showed no significant difference in population stratification between the case and control samples used in the GWAS (Fig E5, *B*). Moreover, Yamaguchi-Kabata et al[E1] reported that the Japanese population stratification mainly divided into 2 clusters, the main islands of Hondo and Ryukyu in Okinawa. They suggested that the false-positive rates in the GWAS would be acceptable when the samples were collected from Hondo island, indicating that the population stratification within that region was relatively small. In this study we collected all of the samples at the single institute in the middle part of Hondo. Consequently, we concluded that there was no significant difference in population stratification between the case and control samples used in the GWAS.

SNP density of the fine-mapping analysis

After applying our QC filter (≥90% call rate per SNP and ≥5% MAF in the case and control samples), the SNPs that we used for the fine-mapping analysis resulted in 52.8% (86/163) of the total number of SNPs for which we initially designed. The major component of eliminated SNPs (76/77) belonged to an MAF of less than 0.05 in our population. Of the passed 86 SNPs, 75 were on the *EP3* gene, with the rest being from the adjacent region. The mean and median lengths between the SNPs on the *EP3* gene were 2.5 and 1.9 kb, respectively. In contrast, the mean and median lengths of the dbSNPs on the *EP3* gene (in total, 76 SNPs with MAFs > 0 based on HapMap-JPT + HapMap-CHB data) were 2.5 and 2.0 kb, respectively, indicating the dense distribution of analyzed SNPs on our custom chip through the gene (Fig E6). Therefore although the success rate was low, the actual coverage of the *EP3* gene by the SNPs that passed the filter was reasonably high enough to satisfy our purpose.

REFERENCE

E1. Yamaguchi-Kabata Y, Nakazono K, Takahashi A, Saito S, Hosono N, Kubo M, et al. Japanese population structure, based on SNP genotypes from 7003 individuals compared to other ethnic groups: effects on population-based association studies. Am J Hum Genet 2008;83:445-56.

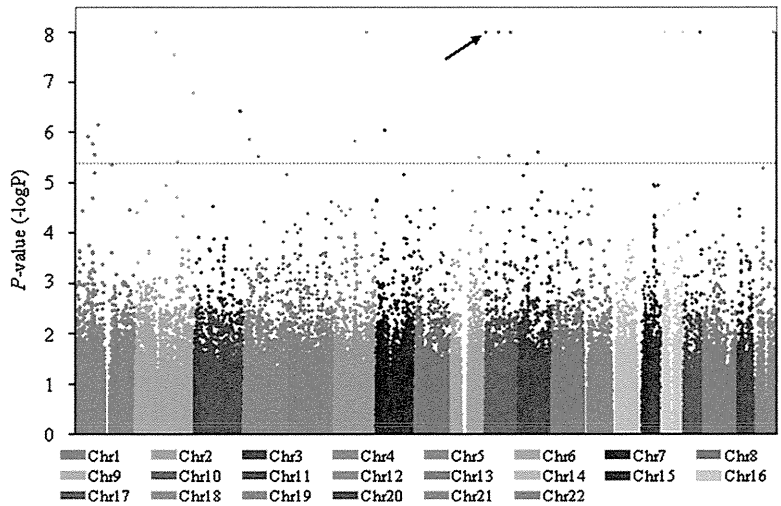

FIG E1. Manhattan plot of the SNPs of the GWAS. Distribution of *P* values obtained from the result of the GWAS is shown. *Horizontal line*, FDR threshold; *arrow*, 2 adjacent SNPs with a similar *P* value were overlapped.

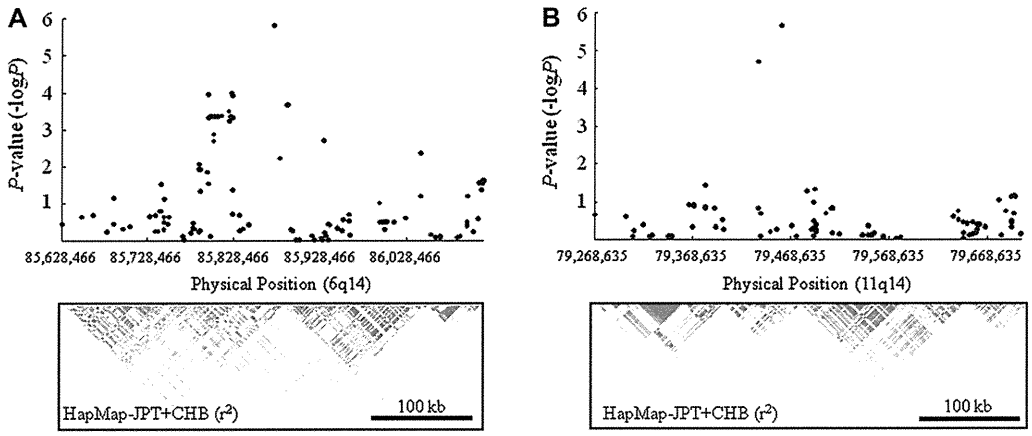

FIG E2. Two other candidate regions associated with SJS/TEN identified by the GWAS. Two other significant SNPs were identified from chromosomes 6 **(A)** and 11 **(B)**. Distribution of *P* values obtained from the result of the GWAS is shown. The LD block for the HapMap-JPT plus HapMap-CHB population based on the r^2 value was obtained from the USCS Genome Browser (http://genome.ucsc.edu/). Physical coordinates refer to National Center for Biotechnology Information Build 35 of the human genome. There was no annotated gene within 500 kb in these regions.

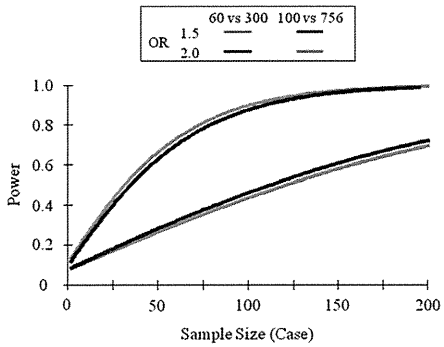

FIG E3. Power calculation. Power calculation was performed by using Power and Sample Size Calculation software (http://biostat.mc.vanderbilt.edu/twiki/bin/view/Main/PowerSampleSize). Power simulations of the maximum number of subjects (100 cases vs 756 control subjects) and the subjects used in the GWAS (60 cases vs 300 control subjects) were performed. The parameters entered were as follows: statistical significance, $P < .05$; MAF, 0.1; and control/case ratio, 5 and 7.56, respectively. *OR*, Odds ratio.

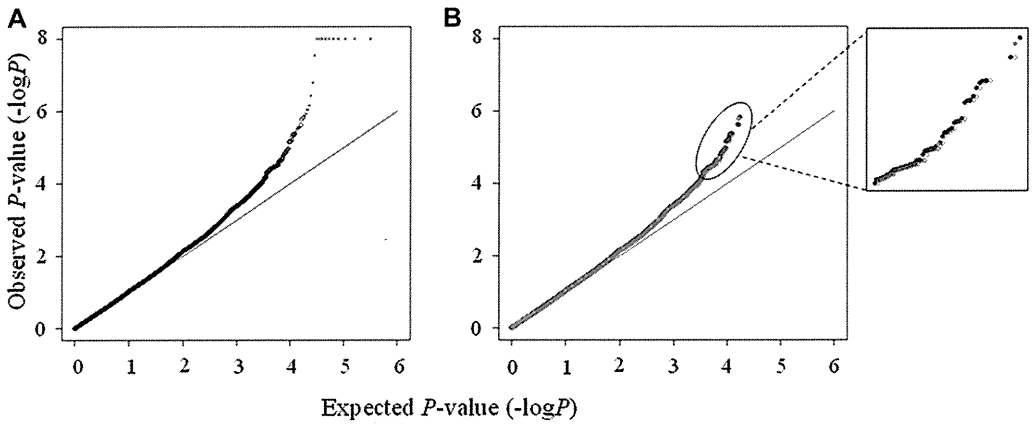

FIG E4. Quantile -quantile plot of the SNPs that passed the stringent filter. **A**, Quantile-quantile plot of the 313,924 SNPs that passed the stringent QC filter in the GWAS and the SNPs selected after the visual check of 2-dimensional cluster plots *(open circles)*. **B**, Distribution of the plot with *(solid black circles)* and without *(open red circles)* the 44 SNPs *(filled blue circles)* derived from the *EP3* region. The distribution of the expected *P* values of genotype frequency comparison plotted against the observed *P* values is shown. Under the null hypothesis, with no disease association, the points lie on the *solid line*. Observed SNP *P* values smaller than 10^{-8} are plotted as 10^{-8}.

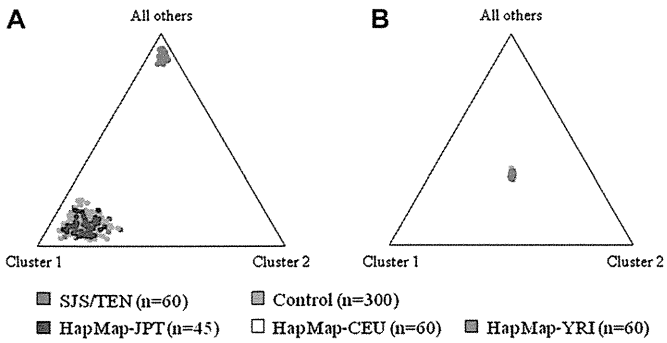

FIG E5. Analysis of population stratification. Population stratification analysis for the subjects used in the GWAS analyzed by using STRUCTURE software is shown. Data are shown in triangle plots (assumed number of populations = 3). **A**, The analysis shows the populations used in the GWAS (case and control groups) and the HapMap-JPT population separated from the HapMap-CEU and HapMap Yoruba in Nigeria (HapMap-YRI) populations with a highest log likelihood of an assumed number of populations of 3. **B**, When the analysis was restricted to the DNA samples used in the GWAS, plots showed a single tight cluster with a highest log likelihood of an assumed number of populations of 1. *Red* and *green dots* correspond to case and control samples, respectively. *Blue*, *yellow*, and *pink dots* correspond to the HapMap-JPT, HapMap-CEU, and HapMap-YRI samples, respectively.

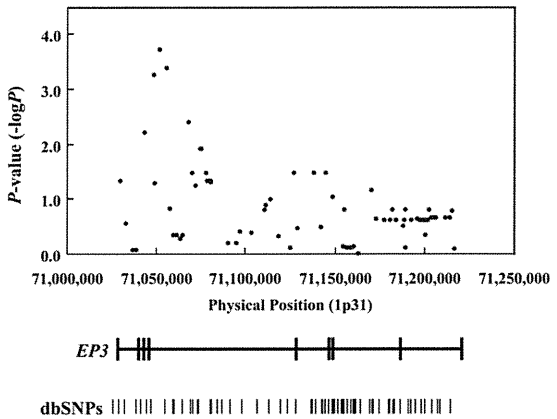

FIG E6. SNP density on the *EP3* gene for the fine-mapping analysis. Density of the *EP3* SNPs (the QC filter passed 75 SNPs) on our custom chip is shown by indicating the distribution of *P* values obtained from the result of the fine-mapping analysis. The exon-intron structure of the *EP3* gene and the dbSNPs on the gene (76 SNPs with MAF > 0 based on HapMap-JPT+CHB data) are shown at the bottom.

TABLE E1. Clinical characteristics of cases and control subjects*

	GWAS		Fine-mapping analysis		Sequencing analysis	
	Cases†	Control subjects	Cases†	Control subjects	Cases†	Control subjects
No. of subjects for case-control analyses	60	300	75	448	100	160
Ratio of female subjects/male subjects	1.1 (60)	1.3 (300)	1.0 (75)	1.8 (448)	1.5 (100)	1.8 (160)
Age‡ (y) at:						
Blood sampling	44.9 ± 17.3 (60)	51.1 ± 13.9 (300)	44.0 ± 16.6 (75)	55.2 ± 14.7 (448)	44.2 ± 17.8 (100)	36.2 ± 11.5 (160)
Onset	29.1 ± 16.7 (60)	—	27.4 ± 17.2 (75)	—	28.0 ± 18.2 (100)	—

*Numbers in parentheses are the total number of subjects whose samples were used for the analysis.
†Many of the case samples were shared in the analyses. We added samples from 15 patients for the fine-mapping analysis to those used in the GWAS, and samples from 25 additional patients were used along with samples from the other 75 patients for the sequencing analysis.
‡Data show the mean ± SD.

TABLE E2. Primers for PCR and sequencing to detect SJS/TEN-associated SNPs

SNPs	Strand	Primers (5′-3′)
rs17131450	Sense	TTTTATGCAGCTTTCGGTCA
	Antisense	CCCCTCCAGGCTGATAACTC
rs5702	Sense	CAAGTAGCAGTTGGCAGCAA
	Antisense	TGCAATCAGACAGGCAAGAG
rs1325949	Sense	AATTGCAAGTCCAGCTCAGG
	Antisense	AGGCCTCAGGGAGCTTTTAC
rs7543182	Sense	TGTGAGGCAAGAACCAGACA
	Antisense	AGGACCTGGGAGGGAAGATA
rs7555874	Sense	AAGCCAGCAAAGGACAAGAA
	Antisense	TGTTGTGTGTCTGCCAGGTT
rs4147114	Sense	TGCTGGAAGCTCATGGTCTA
	Antisense	TGCATGGTTCGTCTAACCTTAT

Gene-expression analysis of polyI:C-stimulated primary human conjunctival epithelial cells

Mayumi Ueta, Katsura Mizushima, Norihiko Yokoi, et al.

Br J Ophthalmol published online July 23, 2010
doi: 10.1136/bjo.2010.180554

BJO Online First, published on July 23, 2010 as 10.1136/bjo.2010.180554

Gene-expression analysis of polyI:C-stimulated primary human conjunctival epithelial cells

Mayumi Ueta,[1,2] Katsura Mizushima,[3] Norihiko Yokoi,[2] Yuji Naito,[3] Shigeru Kinoshita[2]

► Supplementary materials are published online only. To view these files please visit the journal online (http://bjo.bmj.com).

[1]Research Center for Inflammation and Regenerative Medicine, Faculty of Life and Medical Sciences, Doshisha University, Doshisha, Kyoto, Japan
[2]Department of Ophthalmology, Kyoto Prefectural University of Medicine, Kyoto, Japan
[3]Department of Molecular Gastroenterology and Hepatology, Kyoto Prefectural University of Medicine, Kyoto, Japan

Correspondence to
Dr Mayumi Ueta, Department of Ophthalmology, Kyoto Prefectural University of Medicine, 465 Kajiicho, Hirokoji, Kawaramachi, Kamigyoku, Kyoto 602-0841, Japan; mueta@koto.kpu-m.ac.jp

Accepted 16 May 2010

ABSTRACT

Background The authors previously reported that human ocular surface epithelium expressed TLR3 and that its ligand polyI:C stimulated the secretion of IL-6, IL-8 and IFN-β. In this study, to examine comprehensive effects of polyI:C stimulation of primary human conjunctival epithelial cells (PHCjECs), the authors performed a gene-expression analysis of the polyI:C-stimulated PHCjECs using oligonucleotide microarrays, GeneChip.

Methods The transcripts upregulated upon polyI:C stimulation in PHCjECs from two individuals were examined using GeneChip. Eleven new upregulated transcripts of interest were confirmed by quantitative real-time PCR (RT-PCR), and seven proteins produced by those transcripts were examined by ELISA or immunoblot analysis in PHCjECs from three other individuals, respectively.

Results GeneChip analysis showed that 150 transcripts were upregulated more than threefold and that 47 transcripts were upregulated more than 10-fold upon polyI:C stimulation in the PHCjECs. Eleven of the 47 upregulated transcripts (CXCL11, RIG-I, IL28A, CXCL10, CCL5, CCL4, MDA5, IL7R, TSLP, CCL20 and ICAM-1) were significantly upregulated upon polyI:C stimulation by quantitative RT-PCR, and the levels of seven proteins of the transcripts CXCL11, CXCL10, CCL5, CCL20, TSLP, RIG-I and MDA5 were confirmed by ELISA or immunoblot analysis to increase significantly in polyI:C-stimulated PHCjECs.

Conclusions Our results might show that TLR3 of conjunctival epithelium could not only induce antiviral innate immune responses but also regulate the allergic reactions.

INTRODUCTION

Innate immunity, the early host defence against microbes, is primarily studied in host immune-competent cells such as macrophages. The ability of cells to recognise pathogen-associated molecular patterns (PAMPs) depends on the expression of a family of Toll-like receptors (TLRs).[1] Macrophages recognise and phagocytose microbes such as bacteria and produce inflammatory cytokines and chemokines, resulting in inflammation. They also activate adaptive immunity. However, it is now clear that the innate immunity of the mucosa in contact with commensal bacteria differs from conventional innate immunity.[2 3] The ocular surface is one of the mucosa in contact with commensal bacteria.

The ocular surface epithelium serves a critical function as the defensive front line of the innate immune system. While the detection of microbes is arguably its most important task, an excessive host defence reaction to endogenous bacterial flora may initiate and perpetuate inflammatory mucosal responses. The healthy ocular surface is not inflammatory, although ocular surface epithelium is in constant contact with bacteria and bacterial products.[2 3] We have shown that human ocular surface epithelial cells, both corneal and conjunctival epithelial cells, respond to viral double-stranded RNA mimic polyinosine-polycytidylic acid (polyI:C) to produce pro-inflammatory cytokines through TLR3, while they fail to respond functionally to lipopolysaccharide, a TLR4 ligand.[2–5]

Furthermore, we have reported that while human ocular surface epithelium harbours messages for most TLRs, TLR3 is the one with the highest expression level. The expression of TLR3 was higher, while that of the other TLRs was lower, in human ocular surface epithelium than human peripheral mononuclear cells.[2–4 6]

TLR3 recognises double-stranded RNA (dsRNA), a component exhibited in the life cycle of most viruses, which is mimicked by polyI:C, a synthetic dsRNA.[7] We have previously reported that human ocular surface epithelium expressed TLR3 and that polyI:C stimulation induced the secretion of inflammatory cytokines such as IL-6, IL-8 and type I IFN such as IFN-β.[2–4] Inflammatory cytokines such as IL-6 are under TLR3/TRIF/NF-κB signalling, and type I IFN are under the control of TLR3/TRIF/IRF-3 signalling. TLR3 is implicated in triggering antiviral immune responses by producing type I IFN and inflammatory cytokines.[8]

Although the TLR family detects PAMPs either on the cell surface or on the lumen of intracellular vesicles such as endosomes or lysosomes, recent studies have shown the existence of a cytosolic detection system for intracellular PAMPs. These cytosolic PRRs include retinoic acid-inducible gene-I (RIG-I)-like receptors (RLRs) and nucleotide-binding oligomerisation domain (NOD)-like receptors (NLRs). RLRs belong to the RNA helicases family that specifically detects RNA species derived from viruses in the cytoplasm and coordinate antiviral programmes via type I IFN induction. RIG-I and MDA5 are RLRs.[8]

Moreover, we found that TLR3 positively regulated the late-phase reaction of experimental allergic conjunctivitis in a mice model; eosinophilic conjunctival inflammation was reduced in TLR3 knock-out (KO) mice and was aggravated in TLR3 Transgenic (Tg) mice.[9] These findings might suggest that TLR3 could induce not only antiviral innate immune responses but also other functions such as regulations of allergic reactions.

In this study, to examine the comprehensive effects of polyI:C, TLR3 ligand, we performed gene-expression analysis of polyI:C-stimulated primary human conjunctival epithelial cells (PHCjECs)

using oligonucleotide microarrays, GeneChip (Affymetrix, Santa Clara, California). Moreover, we confirmed the upregulation of the transcripts of interest by quantitative real-time PCR (RT-PCR) and ELISA or immunoblot analysis.

MATERIALS AND METHODS

PHCjECs

This study was approved by the institutional review board at Kyoto Prefectural University of Medicine, Kyoto, Japan, and all experimental procedures were conducted in accordance with the tenets of the Declaration of Helsinki. Written informed consent was obtained from all patients after they were given a detailed explanation of the purpose of the research and the experimental protocols.

For GeneChip analysis, quantitative RT-PCR and ELISA, PHCjECs were harvested from conjunctival tissue obtained at the time of conjunctivochalasis surgery and then cultured using a previously described method.[6] Briefly, conjunctival tissues were washed and immersed for 1 h at 37°C in 1.2 U/ml of purified dispase (Roche Diagnostic, Basel, Switzerland), and epithelial cells were detached, collected and cultured in low-calcium defined keratinocyte-SFM medium with defined growth-promoting additives (Invitrogen, Carlsbad, California) including insulin, epidermal growth factor, fibroblast growth factor and 1% antibiotic–antimycotic solution. By using this method, the cell colonies usually became visible within 3 to 4 days. After reaching 80% confluence in 7 to 10 days, the cultured PHCjECs were used in subsequent procedures.

Gene-expression analysis

We previously found that stimulation with polyI:C elicited elevated mRNA expression of IL-6, IL-8 and IFN-β in PHCjECs[3] as well as in primary human corneal epithelial cells.[4] We performed a time-course study of mRNA expression of IL-6, IL-8 and IFN-β, and found that 3 h is the optimal culture time for the polyI:C-treated PHCjECs to induce IL-6-, IL-8- and IFN-β-specific mRNA expression. Thus, to examine the comprehensive effects of polyI:C stimulation of PHCjECs, we performed a gene-expression analysis of PHCjECs from two individuals who were, or were not, cultured with 25 μg/ml polyI:C for 3 h.

Gene-expression profiles were investigated using a high-density oligonucleotide probe array, GeneChip, of Human Genome U133 Plus 2.0 (Affymetrix), which offers a comprehensive analysis of genome-wide expression on a single array and analyses the expression level of over 47 000 transcripts and variants, including 38 500 well-characterised human genes, which comprise more than 54 000 probe sets.

Total RNA was extracted using the Qiagen RNeasy kit (Qiagen, Valencia, California). cRNA preparation and target hybridisation were carried out in accordance with the Affymetrix GeneChip technical protocol. The DNA chips were scanned with a specially designed confocal scanner (GeneChip Scanner 3000; Affymetrix). Array data analysis was performed using Affymetrix GeneChip operating software (GCOS) version 1.0 (Affymetrix); this software analyses image data and computes an intensity value for each probe cell. To quantify RNA abundance, the average-difference values (ie, gene-expression levels) representing the perfect match–mismatch for each gene-specific probe family were calculated, and the fold-changes in the average-difference values were determined in accordance with Affymetrix algorithms and procedures.

Quantitative RT-PCR

Total RNA was isolated from PHCjECs using RNeasy Mini kit (Qiagen) according to the manufacturer's instructions. For the RT reaction, we used the SuperScript Preamplification kit (Invitrogen). Quantitative RT-PCR was performed using an ABI-prism 7700 (Applied Biosystems, Foster City, California) according to a previously described protocol[4] and the manufacturer's instructions. The initial amount of RNA used for reverse transcribing to cDNA was 2 μg in a total volume of 20 μl, and the cDNA was used at twofold dilution for quantitative RT-PCR. The primers and probes were purchased from Applied Biosystems; Assay ID: CXCL11 (Hs00171138_m1), RIG-I (Hs00204833_m1), IL28A (Hs00820125_g1), CXCL10 (Hs00171042_m1), CCL5 (Hs00174575_m1), CCL4 (Hs99999148_m1), MDA5 (Hs00223420_m1), IL7R (Hs00233682_m1), TSLP (Hs00263639_m1), CCL20 (Hs00355476_m1) and ICAM-1 (Hs00277001_m1). To amplify cDNA, PCR was performed in a 25 μl total volume that contained a 1 μl of cDNA template in 2×TaqMan universal PCR master mix (Applied Biosystems) at 50°C for 2 min and 95°C for 10 min, followed by 40 cycles at 95°C for 15 s and 60°C for 1 min. The results were analysed with sequence detection software (Applied Biosystems). The quantification data were normalised to the expression of the housekeeping gene GAPDH. We confirmed the upregulation of transcripts by quantitative RT-PCR three times using PHCjECs derived from different individual, respectively.

ELISA

We performed ELISA to confirm the protein productions. The amounts of CXCL11, CXCL10, CCL5, CCL20 and TSLP released into the culture supernatant were determined by ELISA using the Human CXCL11, CXCL10, CCL5, CCL20 and TSLP DuoSet (R&D Systems, Minneapolis, Minnesota) in accordance with the manufacturer's instructions. Briefly, first, microplates were precoated with capture antibody. Samples and standards were added, and any analyte present was bound by the immobilised antibody. Unbound materials were washed away. Second, biotinylated antibodies were added and bound to the captured analyte. Unbound detection antibodies were then washed away. Third, streptavidin-HRP was used to bind to the detection antibody. Unbound streptavidin-HRP was then washed away. Fourth, tetramethylbenzidine (TMB) substrate solution was added to the wells and a blue colour developed in proportion to the amount of analyte present in the sample. Colour development was stopped with sulfuric acid turning the colour in the wells to yellow. The absorbance of the colour at 450 nm was measured.

Immunoblot analysis of RIG-I and MDA5 protein expression

The RIG-I and MDA5 protein expression in the PHCjECs was examined by immunoblot analysis. PHCjECs were incubated with 10 μg/ml of polyI:C for 12 h, then washed twice and lysed by scrapping in 0.2 ml of an ice-cold CelLytic *M* Cell Lysis Reagent (Sigma-Aldrich Corp., St Louis, Missouri, USA). SDS-polyacrylamide gel electrophoresis was performed using the NuPAGE electrophoresis system (Invitrogen) according to the manufacturer's instructions. The separated proteins were transferred to a polyvinylidene difluoride membrane using the iBlot Gel Transfer Device (Invitrogen) according to the manufacturer's instructions. The membrane was incubated in 5% skim milk with 0.1% Tween 20/TBS buffer for 1 h at room temperature for blocking, then subjected to immunoblot analysis with rabbit anti-RIG-I or rabbit anti-MDA5 antibodies (Cell Signalling Technology, Danvers, Massachusetts, USA) for first antibodies and HRP-conjugated donkey antirabbit IgG antibodies (GE Healthcare, Little Chalfont, UK) for second antibodies. For the detection of the proteins, the ECL Plus Western Blotting Detection System (GE Healthcare) was used.

Ueta M, Mizushima K, Yokoi N, *et al*. *Br J Ophthalmol* (2010). doi:10.1136/bjo.2010.180554

Table 1 Transcripts upregulated more than 10-fold upon polyI:C stimulation of primary human conjunctival epithelial cells

Gene symbol (gene title)	Probe set ID	Ratio (polyI:C+/polyI:C−) Case 1	Case 2
CXCL11 (chemokine (C-X-C motif) ligand 11)	210163_at	1663	512
	211122_s_at	512	1261
IFNB1 (interferon, beta 1, fibroblast)	208173_at	1552	588
DDX58 (=RIG-I) (DEAD (Asp-Glu-Ala-Asp) box polypeptide 58)	218943_s_at	416	52
	222793_at	69	30
IL28A (interleukin 28A)	1552915_at	338	446
	1552609_s_at	91	84
CXCL10 (chemokine (C-X-C motif) ligand 10)	204533_at	338	338
IRF1 (interferon regulatory factor 1)	238725_at	338	23
	202531_at	28	15
IFIT2 (interferon-induced protein with tetratricopeptide repeats 2)	217502_at	315	676
	226757_at	274	194
CCL5 (chemokine (C-C motif) ligand 5)	1405_i_at	239	111
	1555759_a_at	104	23
	204655_at	42	91
IFIT1 (interferon-induced protein with tetratricopeptide repeats 1)	203153_at	208	223
IFIT3 (interferon-induced protein with tetratricopeptide repeats 3)	229450_at	156	84
	204747_at	111	84
CCL4 (chemokine (C-C motif) ligand 4)	204103_at	128	388
SOD2 (superoxide dismutase 2, mitochondrial)	215078_at	119	338
TNF (tumour necrosis factor)	207113_s_at	91	24
IL8 (interleukin 8)	211506_s_at	74	49
	202859_x_at	45	20
CH25H (cholesterol 25-hydroxylase)	206932_at	69	274
IL6 (interleukin 6)	205207_at	64	37
OASL (2′-5′-oligoadenylate synthetase-like)	205660_at	60	158
	210797_s_at	56	74
GBP4 (guanylate binding protein 4)	235574_at	60	32
RHEBL1 (Ras homologue enriched in brain like 1)	1570253_a_at	56	34
IFI44 (interferon-induced protein 44)	214453_s_at	56	17
	214059_at	11	42
IL1F9 (interleukin 1 family, member 9)	220322_at	49	23
CX3CL1 (chemokine (C-X3-C motif) ligand 1)	823_at	49	12
	203687_at	42	16
IFIH1 (=MDA5) (interferon induced with helicase C domain 1)	216020_at	45	11
	1555464_at	20	16
	219209_at	18	16
IL7R (interleukin 7 receptor)	205798_at	42	20
	226218_at	14	16
RSAD2 (radical S-adenosyl methionine domain containing 2)	213797_at	39	294
	242625_at	26	84
IL29 (interleukin 29)	1552917_at	37	169
PMAIP1 (phorbol-12-myristate-13-acetate-induced protein 1)	204286_s_at	37	26
	204285_s_at	37	15
CCL3 (chemokine (C-C motif) ligand 3)	205114_s_at	34	169
TSLP (thymic stromal lymphopoietin)	235737_at	34	52
TNFAIP6 (tumour necrosis factor, alpha-induced protein 6)	206026_s_at	34	20
NIACR2 (niacin receptor 2)	205220_at	32	16
RND1 (Rho family GTPase 1)	210056_at	30	45
HERC5 (HECT domain and RLD 5)	219863_at	30	28
ISG15 (ISG15 ubiquitin-like modifier)	205483_s_at	28	28
TNFAIP3 (tumour necrosis factor, alpha-induced protein 3)	202643_s_at	28	26
	202644_s_at	26	21
CCL20 (chemokine (C-C motif) ligand 20)	205476_at	24	39
ZC3HAV1 (zinc finger CCCH-type, antiviral 1)	220104_at	24	23
CMPK2 (cytidine monophosphate (UMP -CMP) kinase2, mitochondrial)	226702_at	20	37
S1PR3 (sphingosine-1-phosphate receptor 3)	231741_at	20	12
MAP3K8 (mitogen-activated protein kinase kinase kinase 8)	205027_s_at	16	14
ICAM1 (intercellular adhesion molecule 1)	202637_s_at	15	11
CFB (complement factor B)	211920_at	14	13
PPP1R15A (protein phosphatase 1, regulatory subunit 15A)	202014_at	13	14
MX1 (myxovirus (flu virus) resistance 1, interferon-inducible protein p78)	202086_at	12	27
ATF3 (activating transcription factor 3)	202672_s_at	11	37
PLAUR (plasminogen activator, urokinase receptor)	210845_s_at	11	18
	211924_s_at	11	20
MARCKSL1 (MARCKS-like 1)	200644_at	11	11

Data analysis

Data were expressed as the mean±SE and evaluated using the Student t test using the Microsoft Excel software program (Microsoft, Seattle, Washington).

RESULTS

Transcripts upregulated more than 10-fold upon polyI:C stimulation of PHCjECs

The GeneChip analysis showed that 150 transcripts were upregulated more than threefold (Supplemental Data 1) and 47 transcripts were upregulated more than 10-fold upon polyI:C stimulation of PHCjECs from two individuals (table 1): 90 and 89 transcripts were upregulated more than 10-fold in each PHCjECs from case 1 and case 2, respectively (data not shown.). Moreover, even though GeneChip analysis removed the effect of the endogenous prostaglandins using indomethacin, the 47 transcripts were upregulated (Supplemental Data 2). The 47 upregulated transcripts included IL-6, IL-8 and IFN-β, which we previously reported as having been induced by polyI:C stimulation of PHCjECs.

Confirmation of the upregulation of transcripts in PHCjECs by quantitative RT-PCR

Furthermore, we performed a time-course study for 11 upregulated transcripts of interest (CXCL11, RIG-I, IL28A, CXCL10, CCL5, CCL4, MDA5, IL7R, TSLP, CCL20 and ICAM-1) and found that 6 h was a better culture time for them than 3 h. Because the common results from two individuals could not sufficiently cancel the effects derived from individual difference, using PHCjECs derived from other three individuals we confirmed the upregulation of transcripts by quantitative RT-PCR. The upregulation of above 11 transcripts of interest in PHCjECs cultured for 6 h was confirmed by quantitative RT-PCR (figure 1).

Confirmation of the protein productions by ELISA

Next, we examined that production of five proteins from these 11 transcripts by ELISA, and the levels of CXCL11, CXCL10,

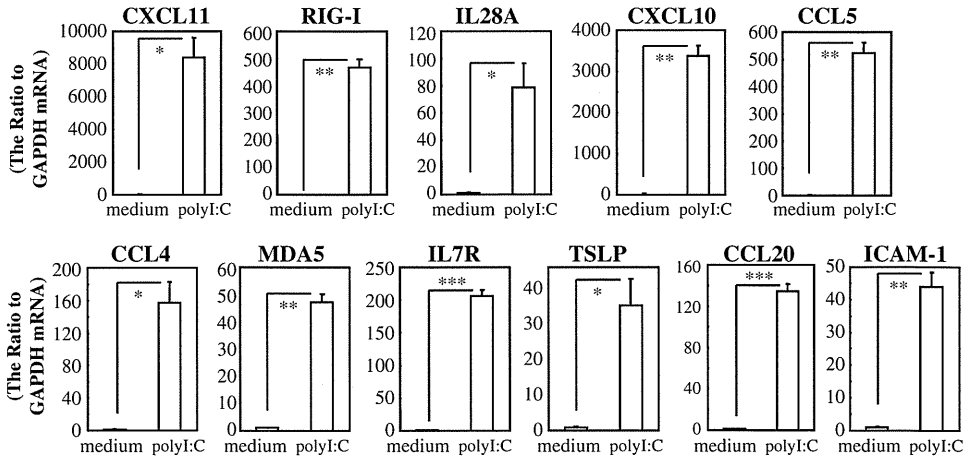

Figure 1 mRNA expression of the 11 transcripts in primary human conjunctival epithelial cells exposed to 25 μg/ml of polyI:C for 6 h. The quantification data were normalised to the expression of the housekeeping gene GAPDH. The y axis shows the increase in specific mRNA over unstimulated samples. Data are representative of three separate experiments and are given as the mean±SEM from one experiment carried out in four wells per group (*p<0.05, **p<0.005, ***p<0.0005).

CCL5, CCL20 and TSLP were found to be increased in PHCjECs cultured with 25 μg/ml of polyI:C for 24 h (figure 2).

Increased expression of TLR3, MDA5 and RIG-I in polyI:C treated PHCjECs

Our results showed that RIG-I and MDA5, which are reportedly implicated in viral dsRNA recognition, are also remarkably upregulated by polyI:C stimulation of PHCjECs. The highest expression of RIG-1 and MDA5 were found at 6 h (figure 3).

Increased protein expression of RIG-I and MDA5

The RIG-I and MDA5 protein expression in the PHCjECs was examined by immunoblot analysis. RIG-I and MDA5 protein expression were detected in PHCjECs incubated with 10 μg/ml of polyI:C for 12 h, but not in PHCjECs without polyI:C (figure 4). These findings show that RIG-I and MDA5 protein expression are upregulated by polyI:C stimulation in PHCjECs.

DISCUSSION

To the best of our knowledge, this is the first report of a study involving gene-expression analysis of polyI:C-stimulated PHCjECs using the oligonucleotide microarrays GeneChip. PolyI:C, a synthetic dsRNA, was reported to be recognised by TLR3, one of the TLRs that recognises molecular patterns associated with microbial pathogens and induces antimicrobial immune responses.[7] Our results showed that 47 transcripts were upregulated more than 10-fold upon polyI:C stimulation of the PHCjECs from two individuals, and the upregulation of 11 transcripts of them (CXCL11, RIG-I, IL28A, CXCL10, CCL5, CCL4, MDA5, IL7R, TSLP, CCL20 and ICAM-1) was confirmed by quantitative RT-PCR.

CXCL11 and CXCL10 have been reported to be expressed principally in response to a wide range of DNA and RNA viruses such as adenovirus,[10] HSV-1,[11] CMV[12] and RSV.[13] Their roles in leucocyte recruitment during inflammation have also been reported.[14] In addition, the levels of CXCL11 and CXCL10 were found to increase in allergic diseases; they increased in the epidermis of AD patients[15] and in the bronchoalveolar lavage fluid of patients with severe asthma.[16]

The three CCL chemokines, CCL4, CCL5 and CCL20, have also been reported to be upregulated during viral infection similarly to CXCL11 and CXCL10.[17] It was also reported that many CCL chemokines including CCL4, CCL5 and CCL20 were upregulated in chronic atopic dermatitis skin lesions.[18]

IL28A and IL29 are two of the IFN-λ proteins that activate IFN-stimulated response elements and induce antiviral activity.[19] The levels of IL28A and IL29 have also been reported to increase in the sputum of patients with asthma.[20]

ICAM-1 is a member of the immunoglobulin superfamily of adhesion molecules and is the ligand of leucocyte functional antigen LFA-1, which is widely expressed on leucocytes. It has been reported that conjunctival epithelial cells were capable of expressing ICAM-1 and that this expression was markedly increased in ocular allergic diseases such as vernal keratoconjunctivitis and allergic atopic keratoconjunctivitis, whereas ICAM-1 was not observed on normal conjunctival epithelial cells.[21]

Thymic stromal lymphopoietin (TSLP) is expressed mainly by barrier epithelial cells and is a potent activator of several cell types, particularly myeloid dendritic cells.[22] TSLP is highly expressed by airway epithelial cells of asthma patients[23] and keratinocytes in skin lesions of patients with atopic dermatitis.[24] IL7R consists of a TSLP receptor complex with a TSLP-binding chain (TSLPR).[22]

Thus, although CXCL11, IL28A, CXCL10, CCL5, CCL4 and CCL20 are innate-immune-response-related genes, they have also been reported to be upregulated in allergic diseases.[15 16 18 20] IL7R, TSLP and ICAM-1 are allergy-related genes. At least nine of the 47 transcripts that were found to be upregulated more than 10-fold upon polyI:C stimulation of the PHCjECs from two individuals might be associated with allergy.

The significant upregulation of these genes, which increases in allergic diseases via polyI:C, might be consistent with our

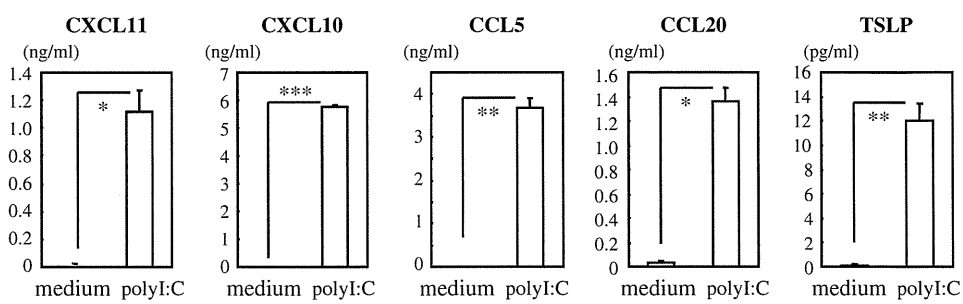

Figure 2 Production of five proteins. Primary human conjunctival epithelial cells were either left untreated or stimulated with 25 μg/ml polyI:C for 24 h. The data are representative of three independent experiments and given as the mean±SEM of four samples (*p<0.05; **p<0.005; ***p<0.0005).

Ueta M, Mizushima K, Yokoi N, *et al. Br J Ophthalmol* (2010). doi:10.1136/bjo.2010.180554

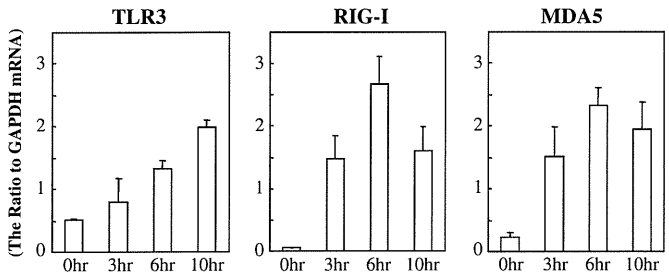

Figure 3 Increased TLR3, RIG-I and MDA5 mRNA expression in polyI:C-stimulated primary human conjunctival epithelial cells. The y axis shows the ratio of mRNA to GAPDH. The time is that poststimulation; the data are given as the mean±SEM of three samples.

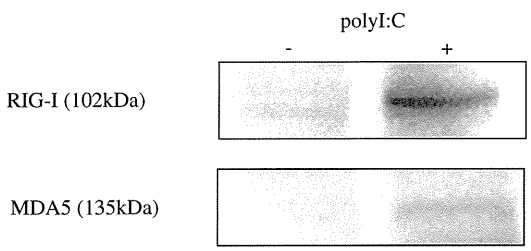

Figure 4 Upregulation of RIG-I and MDA5 protein expression by polyI:C stimulation in primary human conjunctival epithelial cells. Data are representative of three independent experiments.

previous finding that TLR3 positively regulates the late-phase reaction of experimental allergic conjunctivitis in a mice model.[9] Our results might show that TLR3 of conjunctival epithelium could not only induce antiviral innate immune responses, but also regulate the allergic reactions.

Elsewhere we have shown that EP3 is expressed in the ocular surface and that the PGE2-EP3 pathway in conjunctival epithelium works as a negative regulator for allergic conjunctivitis.[25] It is evident that ocular surface epithelial cells regulate the inflammation of allergic conjunctivitis. The actual role of conjunctival epithelium in conjunctival inflammation must be investigated further.

On the other hand, our results showed that RIG-I and MDA5, which are reportedly implicated in viral dsRNA recognition, are also remarkably upregulated by polyI:C stimulation of PHCjECs. We previously reported that TLR3 was the most intensely expressed among TLR1-10 in ocular surface epithelial cells[2–4 6] and speculated that TLR3 mainly contributes to polyI:C inducible responses in ocular surface epithelial cells. However, in this study we found that new receptors that recognise dsRNA and polyI:C, RIG-I and MDA5, are also expressed in PHCjECs and are upregulated by polyI:C stimulation. Of the 10 TLRs identified in humans, TLR3 has been identified to respond to dsRNA. On the other hand, it is notable that the cytoplasmic helicase proteins RIG-I (retinoic-acid-inducible protein I; also known as Ddx58) and MDA5 (melanoma-differentiation-associated gene 5; also known as Ifih1) have been implicated in viral dsRNA recognition; RIG-I and MDA5 were found to detect RNA viruses and polyI:C, as well as TLR3.[8] Further investigation is required to resolve how these receptors contribute to polyI:C-inducible responses.

Studies are also under way in our laboratory to investigate other genes except above 11 transcripts of the 47 transcripts.

In summary, we demonstrated that human conjunctival epithelial cells might be induced to express many transcripts, including not only antiviral innate immune response-related genes but also allergy-related genes, by polyI:C stimulation.

Acknowledgements We thank C Endo for technical assistance.

Funding This work was supported in part by grants-in-aid for scientific research from the Japanese Ministry of Health, Labour and Welfare, the Japanese Ministry of Education, Culture, Sports, Science and Technology, CREST from JST, a research grant from the Kyoto Foundation for the Promotion of Medical Science, the Intramural Research Fund of Kyoto Prefectural University of Medicine and a research grant from the Japan Allergy Foundation.

Competing interests None.

Ethics approval Ethics approval was provided by the institutional review board at Kyoto Prefectural University of Medicine, Kyoto, Japan, and all experimental procedures were conducted in accordance with the tenets of the Declaration of Helsinki.

Provenance and peer review Not commissioned; externally peer reviewed.

REFERENCES

1. **Akira S.** Toll-like receptor signaling. *J Biol Chem* 2003;**278**:38105–8.
2. **Ueta M.** Innate immunity of the ocular surface and ocular surface inflammatory disorders. *Cornea* 2008;**1**(27 Suppl):S31–40.
3. **Ueta M,** Kinoshita S. Innate immunity of the ocular surface. *Brain Res Bull* 2010;**81**:219–28.
4. **Ueta M,** Hamuro J, Kiyono H, *et al*. Triggering of TLR3 by polyI: C in human corneal epithelial cells to induce inflammatory cytokines. *Biochem Biophys Res Commun* 2005;**331**:285–94.
5. **Ueta M,** Nochi T, Jang MH, *et al*. Intracellularly expressed TLR2s and TLR4s contribution to an immunosilent environment at the ocular mucosal epithelium. *J Immunol* 2004;**173**:3337–47.
6. **Kojima K,** Ueta M, Hamuro J, *et al*. Human conjunctival epithelial cells express functional Toll-like receptor 5. *Br J Ophthalmol* 2008;**92**:411–16.
7. **Alexopoulou L,** Holt AC, Medzhitov R, *et al*. Recognition of double-stranded RNA and activation of NF-kappaB by Toll-like receptor 3. *Nature* 2001;**413**:732–8.
8. **Kawai T,** Akira S. The roles of TLRs, RLRs and NLRs in pathogen recognition. *Int Immunol* 2009;**21**:317–37.
9. **Ueta M,** Uematsu S, Akira S, *et al*. Toll-like receptor 3 enhances late-phase reaction of experimental allergic conjunctivitis. *J Allergy Clin Immunol* 2009;**123**:1187–9.
10. **Harvey SA,** Romanowski EG, Yates KA, *et al*. Adenovirus-directed ocular innate immunity: the role of conjunctival defensin-like chemokines (IP-10, I-TAC) and phagocytic human defensin-alpha. *Invest Ophthalmol Vis Sci* 2005;**46**:3657–65.
11. **Carr DJ,** Chodosh J, Ash J, *et al*. Effect of anti-CXCL10 monoclonal antibody on herpes simplex virus type 1 keratitis and retinal infection. *J Virol* 2003;**77**:10037–46.
12. **Cheeran MC,** Hu S, Sheng WS, *et al*. CXCL10 production from cytomegalovirus-stimulated microglia is regulated by both human and viral interleukin-10. *J Virol* 2003;**77**:4502–15.
13. **Bitko V,** Garmon NE, Cao T, *et al*. Activation of cytokines and NF-kappa B in corneal epithelial cells infected by respiratory syncytial virus: potential relevance in ocular inflammation and respiratory infection. *BMC Microbiol* 2004;**4**:28.
14. **Farber JM.** Mig and IP-10: CXC chemokines that target lymphocytes. *J Leukoc Biol* 1997;**61**:246–57.
15. **Klunker S,** Trautmann A, Akdis M, *et al*. A second step of chemotaxis after transendothelial migration: keratinocytes undergoing apoptosis release IFN-gamma-inducible protein 10, monokine induced by IFN-gamma, and IFN-gamma-inducible alpha-chemoattractant for T cell chemotaxis toward epidermis in atopic dermatitis. *J Immunol* 2003;**171**:1078–84.
16. **Ying S,** O'Connor B, Ratoff J, *et al*. Expression and cellular provenance of thymic stromal lymphopoietin and chemokines in patients with severe asthma and chronic obstructive pulmonary disease. *J Immunol* 2008;**181**:2790–8.
17. **Prehaud C,** Megret F, Lafage M, *et al*. Virus infection switches TLR-3-positive human neurons to become strong producers of beta interferon. *J Virol* 2005;**79**:12893–904.
18. **Gros E,** Bussmann C, Bieber T, *et al*. Expression of chemokines and chemokine receptors in lesional and nonlesional upper skin of patients with atopic dermatitis. *J Allergy Clin Immunol* 2009;**124**:753–60.
19. **Kotenko SV,** Gallagher G, Baurin VV, *et al*. IFN-lambdas mediate antiviral protection through a distinct class II cytokine receptor complex. *Nat Immunol* 2003;**4**:69–77.
20. **Bullens DM,** Decraene A, Dilissen E, *et al*. Type III IFN-lambda mRNA expression in sputum of adult and school-aged asthmatics. *Clin Exp Allergy* 2008;**38**:1459–67.
21. **Hingorani M,** Calder VL, Buckley RJ, *et al*. The role of conjunctival epithelial cells in chronic ocular allergic disease. *Exp Eye Res* 1998;**67**:491–500.
22. **Ziegler SF,** Liu YJ. Thymic stromal lymphopoietin in normal and pathogenic T cell development and function. *Nat Immunol* 2006;**7**:709–14.
23. **Ying S,** O'Connor B, Ratoff J, *et al*. Thymic stromal lymphopoietin expression is increased in asthmatic airways and correlates with expression of Th2-attracting chemokines and disease severity. *J Immunol* 2005;**174**:8183–90.
24. **Soumelis V,** Reche PA, Kanzler H, *et al*. Human epithelial cells trigger dendritic cell mediated allergic inflammation by producing TSLP. *Nat Immunol* 2002;**3**:673–80.
25. **Ueta M,** Matsuoka T, Narumiya S, *et al*. Prostaglandin E receptor subtype EP3 in conjunctival epithelium regulates late-phase reaction of experimental allergic conjunctivitis. *J Allergy Clin Immunol* 2009;**123**:466–71.

Lattice Corneal Dystrophy Type IV (p.Leu527Arg) Is Caused by a Founder Mutation of the *TGFBI* Gene in a Single Japanese Ancestor

Hideki Fukuoka,[1] *Satoshi Kawasaki,*[1] *Kenta Yamasaki,*[1] *Akira Matsuda,*[2] *Akiko Fukumoto,*[1] *Akira Murakami,*[2] *and Shigeru Kinoshita*[1]

Purpose. Lattice corneal dystrophy (LCD) type IV (LCD4) is a late-onset corneal dystrophy with amyloid deposition at the deep stromal layer of cornea. As with other corneal dystrophies, this LCD subtype is also caused by a mutation (p. Leu527Arg) of the transforming growth factor, β-induced (*TGFBI*) gene. Although LCD type I has been reported worldwide, LCD4 has been reported only in the Japanese population. In the present study, a haplotype analysis was performed to investigate whether this LCD subtype is caused by a founder mutation.

Methods. Genomic DNA samples were extracted from 13 unrelated patients with LCD4. As a control, genomic DNA samples from 96 normal volunteers were also analyzed. For the haplotype analysis, the samples were amplified by polymerase chain reaction (PCR), TA-cloned, isothermally amplified, and subjected to a 1-base primer extension assay against a mutation site (c.1580T>G) and six known single-nucleotide polymorphisms (SNPs; rs4669, rs2072239, rs7727725, rs17689879, rs6871571, and rs3792900), which are located adjacent to the mutation site.

Results. The haplotype analysis revealed that all the disease-carrying alleles from the 13 LCD4 patients shared an identical haplotype, whereas non-disease-carrying alleles from the normal volunteers and the LCD4 patients exhibited four haplotypes. There was a statistically significant difference in the haplotype distribution between the disease-carrying and the non-disease-carrying alleles.

Conclusions. The findings of this study strongly indicate that LCD4 was caused by a founder mutation of the *TGFBI* gene that occurred in a single Japanese ancestor. (*Invest Ophthalmol Vis Sci.* 2010;51:4523–4530) DOI:10.1167/iovs.10-5343

Cornea is one of the most transparent tissues in the body, and a substantial number of genes contribute to the attainment and maintenance of the specific properties of this tissue.[1,2] Recent advances in molecular biology have allowed us to understand corneal physiology and disease at the molecular level. One of the prominent events in this research area is the discovery of the transforming growth factor, β-induced (*TGFBI*) gene as a causative gene in five classic autosomal dominant corneal dystrophies.[3] Subsequently, other types of inherited corneal dystrophies, such as Meesmann corneal dystrophy (MECD)[4,5] and gelatinous droplike corneal dystrophy (GDLD),[6,7] have been reported.

Lattice corneal dystrophy (LCD) is characterized by stromal amyloid depositions that typically appear as a network or lattice. LCD type I (LCD1) is one of the five dominant *TGFBI*-related corneal dystrophies with characteristic latticelike refractile lines within the corneal stroma.[8] Other than this common LCD, several minor ones have been reported in the *TGFBI* gene (currently designated as Variant LCD in the IC3D classification) that are caused by different mutations.[9] LCD type IV (LCD4, a variant LCD) is one such corneal dystrophy first reported in 1998 as a late-onset LCD with characteristic amyloid depositions located at the deep stromal layer of cornea.[10] Although LCD1 has been reported world-wide,[3,11] LCD4 has been reported only in the Japanese population.[12–19] Thus, some researchers have theorized that LCD4 may be caused by a founder mutation that occurred in a Japanese ancestor.[20]

In this study, we performed a haplotype analysis on genomic DNA samples obtained from 13 patients with LCD4 to investigate this theory. We found that all the disease-carrying alleles of the investigated 13 LCD4 patients shared an identical haplotype around its causative mutation, whereas healthy alleles exhibited four haplotypes with no apparent preference. These data strongly suggest that all LCD4 mutations descend from a founder mutation that occurred in a single Japanese ancestor.

Materials and Methods

Human Samples

Peripheral blood was obtained from 13 patients from 13 unrelated families who had received a clinical diagnosis of LCD4. These 13 patients were 7 men and 6 women, ranging in age from 52 to 83 years (mean age, 69.8). Seven resided in Kyoto, one in Osaka, one in Mie, one in Niigata, one in Kanagawa, and two in Tokyo Prefecture (Fig. 1). Genomic DNA samples from 96 normal Japanese volunteers (48 men and 48 women) were obtained from a research-resource bank (Human Science Research Resource Bank, Osaka, Japan). Written informed consent was obtained from all patients after they were given a detailed explanation of the study protocols. The study adhered to the tenets of the Declaration of Helsinki and was approved by the Institutional Committee for Ethical Issues at Kyoto Prefectural University of Medicine.

Mutation Analysis

Genomic DNA samples were extracted from the peripheral blood of all 13 LCD4 patients by using a commercially available, standard column-

From the [1]Department of Ophthalmology, Kyoto Prefectural University of Medicine, Kyoto, Japan; and [2]Department of Ophthalmology, Juntendo University, Tokyo, Japan.

Supported by Grant-in-Aid 21592238 from the Japanese Ministry of Education, Science, Culture, and Sports, and a grant from the Japanese Ministry of Health, Labor, and Welfare. This work was also supported by a research fund from the Kyoto Foundation for the Promotion of Medical Science.

Submitted for publication February 8, 2010; revised March 12, 2010; accepted March 14, 2010.

Disclosure: **H. Fukuoka**, None; **S. Kawasaki**, None; **K. Yamasaki**, None; **A. Matsuda**, None; **A. Fukumoto**, None; **A. Murakami**, None; **S. Kinoshita**, None

Corresponding author: Satoshi Kawasaki, Department of Ophthalmology, Kyoto Prefectural University of Medicine, 465 Kajii-cho, Hirokoji-agaru, Kawaramachi-dori, Kamigyo-ku, Kyoto 602-0841, Japan; bluenova@koto.kpu-m.ac.jp.

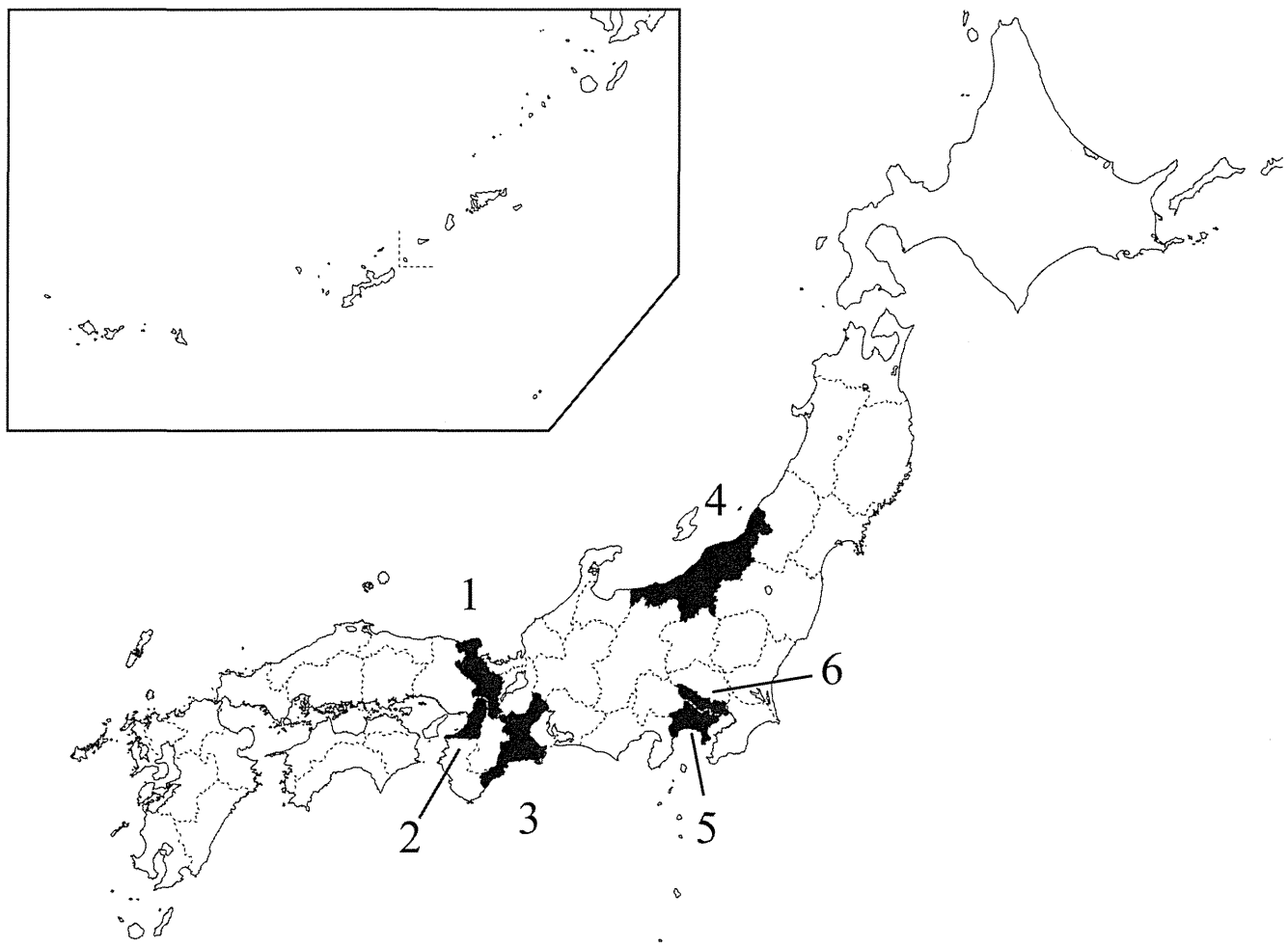

FIGURE 1. Geographic distribution of the residences of the 13 LCD4 patients. Prefectures of residence are shown in *black* and marked as 1, Kyoto; 2, Osaka; 3, Mie; 4, Niigata; 5, Kanagawa; and 6, Tokyo.

based kit (DNeasy Blood & Tissue Kit; Qiagen, GmbH, Hilden, Germany). The samples were then quantitated by the use of a spectrophotometer (NanoDrop; Thermo Fisher Scientific, Inc., Wilmington, DE) and electrophoresed on a 1% agarose gel, to check their integrity. Next, the samples were amplified by polymerase chain reaction (PCR) with primer pairs (Table 1) against the mutation hot spots (exons 4, 11,

TABLE 1. List of the Oligomers

Oligomer	Target	Purpose	Direction	Sequence
Exon4_F	TGFBI	PCR	Forward	CCCCAGAGGCCATCCCTCCT
Exon4_R	TGFBI	PCR	Reverse	CCGGGCAGACGGAGGTCATC
Exon11_F	TGFBI	PCR	Forward	CTCGTGGGAGTATAACCAGT
Exon11_R	TGFBI	PCR	Reverse	TGGGCAGAAGCTCCACCCGG
Exon12_F	TGFBI	PCR	Forward	GACAGGTGACATTTTCTGTGT
Exon12_R	TGFBI	PCR	Reverse	GATCACTACTTTAGAAAAATG
Exon13_R	TGFBI	PCR	Reverse	GCTGCAACTTGAAGGTTGTG
TGFBI_27889	c.1580	1-Base primer extension	Forward	TGCCATCCAGTCTGCAGGAC
TGFBI_27929	rs4669	1-Base primer extension	Forward	TTTTTTTTTTGAAGGAGTCTACACAGTCTT
TGFBI_28010	rs2072239	1-Base primer extension	Forward	TTTTTTTTTTTTTTGTAAAGACCAACTTAAGTACAC
TGFBI_28238	rs7727725	1-Base primer extension	Forward	TTTTTTTTTTTTTTTTTTTTTTTTCAGGAACCAGGGAGGTCA
TGFBI_28641	rs17689879	1-Base primer extension	Forward	TTTTTTTTTTTTTTTTTTTTTTTTTTTTGGCAGGGGATCTAGTGGTTA
TGFBI_28700	rs6871571	1-Base primer extension	Forward	TTTTTTTTTTTTTTTTTTTTTTTTTTTTTTTTTTTCAGCCTGTGTTGGGAGGATT
TGFBI_29257	rs3792900	1-Base primer extension	Forward	TTTTTTTTTTTTTTTTTTTTTTTTTTTTTTTTTTTTTTTTTTGTGTTAGAGGTTGGTACAGG

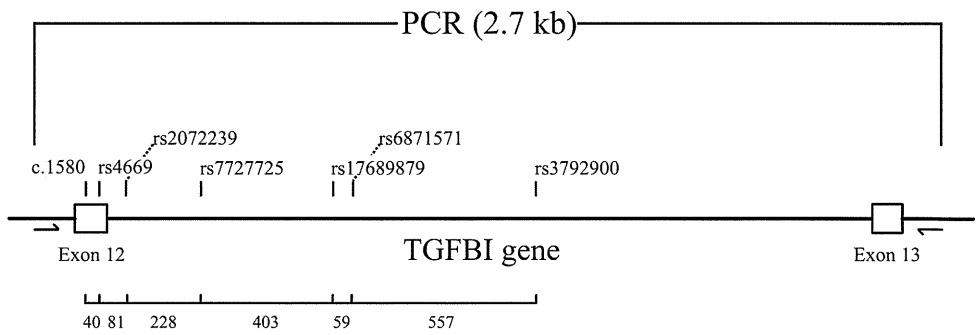

FIGURE 2. The genomic structure for the *TGFBI* gene with sites of mutation and SNPs investigated. *Arrows*: PCR primers that amplify a fragment containing all the SNP and mutation sites. The physical distance between two neighboring SNPs is also indicated in base lengths at the *bottom*.

and 12) of the *TGFBI* gene. The amplified products were then treated with a mixture of exonuclease I and shrimp alkaline phosphatase (ExoSAP-IT; GE Health Care, Ltd., Little Chalfont, UK) to digest residual dNTP and primer. The amplified products were then subjected to sequencing reaction (BigDye Terminator ver. 3.1 Cycle Sequencing Kit; Applied Biosystems, Inc. [ABI], Foster City, CA), and the products were electrophoresed on an automated sequencer (3130xl Genetic Analyzer; ABI). The sequence data were analyzed through the use of commercially available alignment software (Variant Reporter; ABI).

Haplotype Analysis

Genomic DNA samples were amplified by PCR using a primer pair (exon12_F and exon13_R; Table 1) against a genomic region between exon 12 and 13 of the *TGFBI* gene, which harbors the site of the c.1580T>G mutation and six known SNPs (Fig. 2, Table 2). The amplified products were then electrophoresed on a 1% agarose gel, excised, purified with a commercially available column-based purification kit (Wizard SV Gel and PCR Clean-Up System; Promega, Madison, WI), and ligated to a TA-cloning vector (pGEM-T Easy Vector; Promega). The plasmid vector was transformed into chemically competent *Escherichia coli* cells (competent high JM-109; Toyobo Co., Ltd., Osaka, Japan) and seeded on a 1% LB agar plate supplemented with IPTG and X-gal for the standard blue-white selection. After 24 hours' incubation, 16 white colonies were picked from each sample and isothermally amplified overnight with a phi29 polymerase-based plasmid amplification kit (Illustra TempliPhi DNA Amplification Kit; GE Health Care). Each of the amplified products was then subjected to a 1-base primer extension assay (SNaPshot; ABI) with seven pooled primers (Table 1) against the sites of the mutation and the six known SNPs. After treatment with shrimp alkaline phosphatase, the assay products were electrophoresed on the automated sequencer, and the data were analyzed with the use of commercially available software (GeneMapper Software; ABI). Because artificial recombination presumably occurring during the PCR amplification and the bacterial transformation is not negligible in this analysis, a Perl-based program (HapTyper.pl) was created to estimate the most probable haplotype pair from the processed data for each sample.

Statistical Analysis

For the identification of the statistical significance in the haplotype distribution between the affected alleles and the nonaffected alleles, χ^2 and Fisher's exact tests were performed with commercially available statistical software (SAS ver. 9.1; SAS Institute Inc., Cary, NC). For the calculation of statistical power, R language (R Foundation, Vienna, Austria) was used.

RESULTS

The enrolled 13 LCD4 patients, except for 1 patient, exhibited similar corneal haze composed of isolated or fused refractile opacities, most of them being dotlike, and some being latticelike. Most important, these depositions were mainly located within the deep stromal layer, which seems to be specific to this disease and of great diagnostic value, as reported previously. Sequencing analysis revealed that all the 13 LCD4 patients enrolled in this study exhibited a substitution mutation (T to G; c.1580T>G), resulting in an amino acid transition from leucine to arginine (p.Leu527Arg; Fig. 3). Only one patient (59-year-old woman) was homozygous for the mutation site, and she exhibited a much more severe corneal phenotype than did other patients heterozygous for the mutation, such as another homozygous LCD4 patient detailed in a previous report.[19] One patient had a heterozygous substitution mutation from A to G at a different nucleotide position (c.1631A>G) that results in an amino acid transition from asparagine to serine (p.Asn544Ser), which has already been reported to be causative of another type of variant LCD.[17,20,21] In this patient, these two mutations were located on different alleles from one another, as determined by subsequence haplotype analysis (data not shown).

Haplotype analysis was performed to examine whether the combination of the six SNPs, which are close to the c.1580T>G mutation and hence show a strong linkage disequilibrium to that mutation site, was identical among the disease-

TABLE 2. List of SNPs within the Amplified Region

Region	rs ID	Heterozygosity	Sequence
Exon12	rs4669*	0.494	CCTCAACCGGGAAGGAGTCTACACAGTCTT (C/T) GCTCCCACAAATGAAGCCTTCCGAGCCCTG
Intron12	rs2072239*	0.294	TGAGGGATCACTACTTTAGAAAAATGGAGA (C/T) GTGTACTTAAGTTGGTCTTTACCCAAGAGT
Intron12	rs7727725*	0.494	GGAGGATGAGAGCAGGAACCAGGGAGGTCA (A/T) GAGCCTTGGACAAGGGCACAGAACAGCAGC
Intron12	rs17689879*	0.444	GAGGATGTTTGGCAGGGGATCTAGTGGTTA (C/T) GGGTGGCTAAGAAAAATGAGGAAGGTAAGA
Intron12	rs6871571*	0.494	GAGTATCTTGCAGCCTGTGTTGGGAGGATT (A/G) AATAGGATGCCACACACAGGGCCAGGCAGA
Intron12	rs58761304	N.D.	GCAGGAATGGGAGTTGCAGTGTTTAGCTCA (G/T) ATGCATGCCTGTGAGAGATGCTTCCACTCT
Intron12	rs3792900*	0.453	TGCATGGGATGTCCTTTCAATATCTCTAAC (A/G) CCTGTACCAACCTCTAACACTCTCTGTCCC
Intron12	rs45583534	0.023	ACTGATGTGGGCTGAAAGGAATGCTGAGAC (A/G) TGACGAGGAGAGATGCTGCGGAGGGAATAT
Intron12	rs41502049	0.076	GAAACATGAGTCATACTCACAGAGGAGTAT (C/G) GATTAACTCCTTCTCAGCAGCCAGGGAGCC
Intron12	rs45474493	0.011	AACCCAGAGGCCAACTGACTGCTGGGGCAG (A/T) TTTGTGGTCATGAACATGTGCTTTGTGTCC

The amplified region is illustrated in Figure 2.
* SNPs investigated.